Time-dependent few-body approaches to nuclear collisions

Aditya S. Tejas [1,*] and Edward C. Simpson [1,**]

[1]Department of Nuclear Physics and Accelerator Applications, The Australian National University, Canberra, Australia.

Abstract. Coupled-channels models for non-relativistic nuclear collisions face challenges in consistently describing fusion cross-sections across a wide range of energies. This work develops the foundations for alternative approaches to fusion using time-dependent few-body methods. We present a robust, numerically convenient time-dependent method for determining the S-matrix via the wave packet time-correlation function, accounting for the long-range Coulomb potential. We briefly review time-dependent scattering theory and the action of Dollard's Coulomb Møller wave operators. We apply the theory to low-energy $\alpha + \alpha$ scattering, and preliminary results show excellent agreement with FRESCO. We highlight the potential of the method to resolve contributions to scattering from different mechanisms, such as resonances.

1 Introduction

Nuclear collisions have many applications in nuclear science, from understanding the complex many-body interactions of nuclei and synthesising new elements, to producing medical isotopes and zero-carbon electricity. Few-body models, such as coupled channels (CC) [1], have been very successful for modelling reactions with small numbers of degrees of freedom, while naturally including tunnelling. Within the coupled-channels framework, fusion has been modelled phenomenologically using an absorbing potential or an incoming-wave boundary condition to remove flux that has penetrated the internuclear potential barrier or the fusion barrier. There is, therefore, no explicit description of the processes that lead to the dissipation of the kinetic energy of the collision into internal degrees of freedom, nor when and where they begin.

Recent experiments from Cook et al. [2] for the scattering of ^{40}Ca + ^{208}Pb have demonstrated that multi-nucleon transfers start occurring at much larger distances than previously understood (extending outside the barrier) and can result in many nuclide pairs with high excitation energies (up to 40 MeV). How this affects fusion is not well understood. These experimental results pose a further challenge to our models of fusion, which already struggle to consistently describe both few-body and fusion reactions over wide ranges of energies [3, 4].

A key distinguishing feature of fusion is that its timescale is much larger than that of elastic scattering and other direct reaction processes. Hence, as an alternative to absorbing boundary conditions, Webber [5] simulated fusion by introducing couplings to multiple reaction channels within the fusion barrier. This caused temporary trapping of flux due to resonances, in the form of quasi-bound states of the potential, that were sufficiently long-lived to be associated with a compound nucleus. Webber's analysis, using the time-dependent coupled channels (TDCC) framework to estimate wave packet barrier transmission, showed promise. However, further work is needed to calculate the energy-resolved scattering S-matrix and obtain reaction observables. In general, time-dependent analysis of quantum collisions can enable us to resolve the contributions to scattering from different reaction mechanisms that have different timescales. This feature may not only allow deeper study of the mechanisms involved in nuclear collisions but also the calculation of fusion cross-sections using models such as the one explored by Webber.

The S-matrix can be calculated using the wave packet time-correlation function method, as introduced by Tannor and Weeks [6] and applied to quantum chemistry problems. Whilst a prior application of the approach to nuclear problems [7] showed promise, it required a curation procedure to fix the resultant phase shifts and extrapolate to low energies. The work presented here is based on Ref. [8], which formally extends the use of the wave packet time-correlation function method to cases where a long-range Coulomb potential is present. Our aim is to develop a robust framework for applying the time-dependent coupled channel (TDCC) method to solve the scattering problem. In addition to this, Ref. [8] discusses how the dynamics of different reaction mechanisms may be inferred through the time-correlation function $C(t)$, which is a Fourier-like transform of the energy-resolved S-matrix $S(E)$. Subsequently, the analysis of $C(t)$, independent of how $S(E)$ is calculated (including static methods), may allow us to extract fusion observables by separating the contribution of long-lived resonant states from other mechanisms.

We begin by reviewing time-dependent wave packet scattering theory in Sec. 2, followed by the theorem to enable the use of this approach when the Coulomb potential is included in Sec. 3. Then in Sec. 4.2 we illustrate the application of the method for low-energy $\alpha + \alpha$ scattering,

*e-mail: adityasingh.tejas@anu.edu.au (corresponding author)
**e-mail: edward.simpson@anu.edu.au

chosen due to the presence of a low-energy 2^+ resonance. For simplicity, only the single-channel case is presented here; the results are easily generalisable to multi-channel scattering [9]. Numerical methods and applications are discussed in Sec. 4, and we summarise in Sec. 5.

2 Time-dependent Scattering Theory

We first give a brief overview of time-dependent scattering theory. For simplicity, we consider the case of spinless and structureless particles. The Hamiltonian H of a quantum system described by a time-independent potential $V(\mathbf{r})$ can be written as $H \equiv H_0 + V(\mathbf{r})$, $\mathbf{r} \in \mathbb{R}^3$, where $H_0 = -\hbar^2\Delta/(2m)$ is the Hamiltonian for a free particle of mass m. H acts in the Hilbert space $\mathcal{H} = L^2(\mathbb{R}^3)$.

Free-particle (generalised) eigenstates $|\Psi^{\mathbf{k}}_{\text{free}}\rangle$ solve the time-independent free Schrödinger equation $(H_0 - E)\,|\Psi^{\mathbf{k}}_{\text{free}}\rangle = 0$, and scattering eigenstates of the system $|\Psi^{\mathbf{k},\pm}_{\text{scat}}\rangle$ solve $(H - E)\,|\Psi^{\mathbf{k},\pm}_{\text{scat}}\rangle = 0$ in the distributional sense. In both cases, $E \equiv \hbar^2|\mathbf{k}|^2/(2m)$ is the free-particle energy, $\mathbf{k}$ labels the asymptotic momentum. Here, $|\Psi^{\mathbf{k},\pm}_{\text{scat}}\rangle$ are the two linearly independent solutions of the relevant Lippmann-Schwinger equations, defined such that, + and − labels correspond to asymptotic boundary conditions of incoming and outgoing spherical waves, respectively [10].

Møller wave operators (provided they exist) map the free eigenstates to the scattering eigenstates. For asymptotically decaying potentials $V(\mathbf{r}) \to 0$ as $|\mathbf{r}| \to \infty$, that decay sufficiently quickly [11] (which does not include the Coulomb potential), standard Møller operators $\Omega^\pm$ exist. That is, $\Omega^\pm : P_{\text{ac}}(H_0)\mathcal{H} \mapsto P_{\text{ac}}(H)\mathcal{H} \equiv \mathcal{R}$, and can be defined as

$$\Omega^\pm \equiv \operatorname*{s-lim}_{t\to\pm\infty} e^{iHt/\hbar}e^{-iH_0t/\hbar}, \tag{1}$$

where $P_{\text{ac}}(H)$ is the projection operator onto the absolutely continuous spectral subspace of H, and $\mathcal{R} = \text{span}(\{|\Psi^{\mathbf{k},\pm}_{\text{scat}}\rangle\})$ for asymptotically complete theories. In the single-channel case $P_{\text{ac}}(H_0)$ is the identity $\mathbb{1}_{\mathcal{H}}$ on $\mathcal{H}$.

To understand the role of Møller operators, suppose that the physical state $e^{-iHt/\hbar}\psi_0$ for $\psi_0 \in \mathcal{R}$ (at some finite $t \equiv 0$) describes the scattering process. Then, for asymptotically convergent theories, it will uniquely map to states $\psi^{f/i} \in \mathcal{H}$ described by free evolution $e^{-iH_0t}\psi^{f/i}$, such that $\psi_0 = \Omega^\pm\psi^{f/i}$. Here labels final ($f$) and initial ($i$) corresponds to + and −, respectively. Hence, the scattering operator S, or the S-matrix, can be defined as $S \equiv (\Omega^+)^\dagger\Omega^-$.

The S-matrix in the momentum representation is given by the overlap:

$$\begin{aligned}\langle\Psi^{\mathbf{k}',+}_{\text{scat}}|\Psi^{\mathbf{k},-}_{\text{scat}}\rangle &= \langle\Psi^{\mathbf{k}'}_{\text{free}}|(\Omega^+)^\dagger\Omega^-|\Psi^{\mathbf{k}}_{\text{free}}\rangle \\ &= \langle\Psi^{\mathbf{k}'}_{\text{free}}|S\,|\Psi^{\mathbf{k}}_{\text{free}}\rangle \equiv S(\mathbf{k}',\mathbf{k})\delta(E-E'),\end{aligned} \tag{2}$$

where $S(\mathbf{k}',\mathbf{k})$ is a scalar-valued function, and the first equality is a consequence of asymptotic convergence and the intertwining property of wave operators $H\Omega^\pm = \Omega^\pm H_0$.

For spherically symmetric potentials $V(\mathbf{r}) \equiv V(r)$, $r \equiv |\mathbf{r}|$, with only two interacting particles in the system, the scattering problem can be reduced to a one-dimensional radial problem using partial wave analysis. Then, the Hilbert space can be decomposed as $\mathcal{H} = \bigoplus_{\ell=0}^\infty \mathcal{H}_\ell$, where $\mathcal{H}_\ell$ are the partial wave Hilbert spaces [12]. The partial wave Hamiltonian is $H_\ell \equiv H_0 + \hbar^2\ell(\ell+1)/(2\mu r^2) + V(r) \equiv H_0^\ell + V(r)$, where $\mu \equiv m_1m_2/(m_1+m_2)$ is the reduced mass in the centre of mass frame of the two particles with masses m_1 and m_2. This condition also implies the existence of simultaneous energy and orbital angular momentum eigenstates $|\Psi^{k,\pm}_{\text{scat},\ell}\rangle$, $k \equiv |\mathbf{k}|$, which solve $(H_\ell - E)\,|\Psi^{k,\pm}_{\text{scat},\ell}\rangle = 0$ and we can impose the orthonormality condition $\langle\Psi^{k',\pm}_{\text{scat},\ell}|\Psi^{k,\pm}_{\text{scat},\ell}\rangle = \delta(k-k')$. Then, the full scattering solution $|\Psi^{\mathbf{k},\pm}_{\text{scat}}\rangle$ in coordinate space can be expanded in the basis of radial wave functions as [13]:

$$\langle\mathbf{r}|\Psi^{\mathbf{k},\pm}_{\text{scat}}\rangle \equiv \frac{4\pi}{kr}\sum_{\ell=0}^{\infty}\sum_{m=-\ell}^{\ell} i^\ell Y_\ell^m(\hat{\mathbf{r}})Y_\ell^{m*}(\hat{\mathbf{k}})\,\langle r|\Psi^{k,\pm}_{\text{scat},\ell}\rangle\,. \tag{3}$$

The partial wave S-matrix in the energy representation (energy-resolved) will be given by $\langle\Psi^{E',+}_{\text{scat},\ell}|\Psi^{E,-}_{\text{scat},\ell}\rangle \equiv S_\ell(E)\delta(E-E')$, where $|\Psi^{E,\pm}_{\text{scat},\ell}\rangle$ are generalised scattering energy eigenstates of H_ℓ. The wave packet time-correlation function formulation to calculate the energy-resolved S-matrix was introduced by Tannor and Weeks [6] (see also Viswanathan et al. [14]) in quantum chemistry. Using this formalism [6, 15], we can write

$$\begin{aligned}S_\ell(E) = \frac{\hbar^2k}{\mu}&\frac{(2\pi\hbar)^{-1}}{\langle\Psi^k_{\text{free},\ell}|\psi^f_\ell\rangle^*\,\langle\Psi^k_{\text{free}}|\psi^i_\ell\rangle} \\ &\times\int_{-\infty}^{\infty}\mathrm{d}t\;\langle\psi^f_\ell|(\Omega^+_\ell)^\dagger e^{-iHt/\hbar}\Omega^-_\ell|\psi^i_\ell\rangle\,e^{iEt/\hbar},\end{aligned} \tag{4}$$

where $|\Psi^k_{\text{free},\ell}\rangle$ solve $(H_\ell^0 - E)\,|\Psi^k_{\text{free},\ell}\rangle = 0$, and $\Omega^\pm_\ell : \mathcal{H}_\ell \mapsto P_{\text{ac}}(H_\ell)\mathcal{H}$ are partial wave Møller operators [12], such that, $\Omega^\pm = \bigoplus_{\ell=0}^\infty \Omega^\pm_\ell$. State vectors $|\psi^{f/i}_\ell\rangle \in L^2$ are the final and initial wave packets, respectively, described by free evolution (defined in the $\{|\Psi^k_{\text{free},\ell}\rangle\}$ basis). These wave packets can be arbitrarily constructed for analytical and numerical convenience [6]. Furthermore, in the above, we can identify the wave packet time-correlation function

$$C_\ell(t) \equiv \langle\psi^f_\ell|(\Omega^+_\ell)^\dagger e^{-iHt/\hbar}\Omega^-_\ell|\psi^i_\ell\rangle\,. \tag{5}$$

We will revisit this object in Sec. 4.3.

3 Møller Operators & the Coulomb Potential

Now, suppose that the scattering system is described purely by the Coulomb potential $V_C(r) = \alpha\hbar cZ_1Z_2/r$, where α is the fine structure constant and Z_1, Z_2 are the charge numbers of the particles. Then, in contrast to the discussions in Sec. 2, $V_C(r)$ is a long-range potential, and consequently standard Møller operators in Eq. (1) do not exist. Dollard [10] proved the existence of modified (Coulomb) Møller operators, given by

$$\Omega^\pm_C \equiv \operatorname*{s-lim}_{t\to\pm\infty} e^{iHt/\hbar}e^{-iH_0t/\hbar - iA(t)}, \tag{6}$$

where $A(t)$ is a time-dependent anomalous operator defined in Ref. [10]. The inclusion of this term accounts for the long-range effects of the Coulomb potential, which causes logarithmic phase distortion in the coordinate space scattering eigenfunctions relative to the free-particle eigenfunctions. Note that these are also the correct

Møller operators for the theory if other short-range potentials, as defined in Sec. 2, are additionally included [16].

It should be evident from Eq. (4) that, to use the formalism, the action of Møller operators needs to be understood. In quantum chemistry applications, where only short-range potentials are present, Zhang and collaborators [17], and Viswanathan et al. [14] were able to omit the application of Møller operators by localising the initial and final wave packets in the asymptotic region of the short-range potentials (where $|V(r)| \to 0$) as the Møller operators act as the identity.

When the Coulomb potential is present $\Omega_C^\pm$ does not act as the identity on the wave packets, even if they are localised in the asymptotic region. Therefore, the application of $\Omega_C^\pm$ can never be omitted. Kröger and collaborators [18] numerically (and approximately) applied the Coulomb Møller operators directly in the momentum space to wave packets in the interaction region and obtained the wave packet to wave packet S-matrix (not using the formalism in Eq. (4)). We initially applied them using time propagation in position space, but found it impractical because of the slow rate of convergence when the Coulomb interaction is strong (i.e., for the collision of heavy nuclei at near-barrier energies).

Therefore, to use the formalism in Eq. (4) efficiently and accurately, we found that $\Omega_C^\pm$ can be applied analytically when the wave packets are localised in the asymptotic region of the short-range potentials present. This can be derived by relating the time-dependent action of Møller operators to their time-independent action as integral transforms, see Marchesin and O'Carroll [16] (see also Green and Lanford [19]) and the references therein.

Theorem 1. Consider a system described by the Hamiltonian $H = H_0^\ell + V(r) + V_C(r)$, where $V(r)$ and $V_C(r)$ are short-range and the Coulomb potentials, respectively. We can then define purely incoming initial $\psi_\ell^i(r) \equiv \langle r|\psi_\ell^i\rangle$ and outgoing final $\psi_\ell^f(r)$ free wave packets, that are localised in the asymptotic region of the short-range potentials (defined to be the region where $|V(r)| \to 0$) as

$$\psi_\ell^{f/i}(r) \equiv \sqrt{\frac{2}{\pi}} \int_0^\infty \mathrm{d}k\, \chi_\ell^{f/i}(k) \Phi_{\mathrm{free},\ell}^{k,\pm}(r). \tag{7}$$

Here, $\Psi_{\mathrm{free},\ell}^k(r) \equiv \Phi_{\mathrm{free},\ell}^{k,-}(r) + \Phi_{\mathrm{free},\ell}^{k,+}(r)$, $+/-$ label the outgoing/incoming waves and correspond to labels f/i, respectively. Then, if the spatial range within which Coulomb Møller operators $\Omega_{C,\ell}^\pm$ act is asymptotic, i.e., the wave packets $\psi_\ell^\pm(r) \equiv (\Omega_{C,\ell}^\pm \psi_\ell^{f/i})(r)$ resulting from the action of respective $\Omega_{C,\ell}^\pm$ remain within the asymptotic region of the short-range potentials, then their action will be given by the integral transforms [9, 16]:

$$\psi_\ell^\pm(r) = \sqrt{\frac{2}{\pi}} \int_0^\infty \mathrm{d}k\, \chi_\ell^{f/i}(k) e^{\mp i\delta_\ell^C(k)} \Phi_{\mathrm{scat},\ell}^{C,k,\pm}(r), \tag{8}$$

where $\Psi_{\mathrm{scat},\ell}^{C,k}(r) \equiv \Phi_{\mathrm{scat},\ell}^{C,k,+}(r) + \Phi_{\mathrm{scat},\ell}^{C,k,-}(r)$ are the regular scattering eigenfunctions of $H = H_0^\ell + V_C(r)$, and $\delta_\ell^C(k)$ is the Coulomb phase shift [13].

Based on the partial wave expansion in Eq. (3), in explicit form, $\Psi_{\mathrm{free},\ell}^{k,\pm}(r) = \pm kx h_\ell^\pm(kx)/(2i)$ and $\Psi_{\mathrm{scat},\ell}^{C,k,\pm}(r) = \pm H_{\ell,\eta}^\pm(kx)/(2i)$, where $h_\ell^\pm(kx)$ and $H_{\ell,\eta}^\pm(kx)$ are the outgoing and incoming spherical Hankel and Coulomb Hankel functions, respectively [13]. The Sommerfeld parameter $\eta(k)$ characterises the strength of the Coulomb interaction.

Remark 1.1. Contrary to the intuitive understanding in the case of repulsive potentials, the action $(\Omega_{C,\ell}^\pm \psi_\ell^{f/i})(r)$ results in $\psi_\ell^\pm(r)$ that are closer to the scattering centre, relative to the position of $\psi_\ell^{f/i}(r)$. This behaviour arises due to the anomalous term $e^{-i\tilde{A}(t)}$ in $\Omega_C^\pm$ (cf. Eq. (6)).

Remark 1.2. The method in Theorem 1 allows us to precisely define the momentum space (and hence energy) distribution of the free wave packets, which is the range over which $S_\ell(E)$ can be numerically determined. However, in general, one may not have the ability to define the position of the scattering wave packets precisely (see Remark 1.1).

Remark 1.3. One can also choose to arbitrarily define the scattering wave packets $\psi_\ell^\pm(r)$ instead and use the inversion of Theorem 1 to compute the momentum space distribution of the associated free wave packets $\chi_\ell^{f/i}(k) = \langle \Psi_{\mathrm{free},\ell}^k | \psi_\ell^{f/i}\rangle$. This allows precise spatial positioning of $\psi_\ell^\pm(r)$; however, the energy distribution of $\psi_\ell^\pm(r)$ will be determined by the calculated $\chi_\ell^{f/i}(k)$. Both approaches give numerically equivalent results [8].

Further details and multi-channel generalisation of the theorem and other concepts will be presented in the forthcoming Ref. [9].

4 Numerical Applications

We now discuss our methods for numerically solving Eq. (4) and its application to the case of $\alpha + \alpha$ scattering.

4.1 Methods

To apply the formulation in Eq. (4), the initial scattering wave packet $\Omega_\ell^- |\psi_\ell^i\rangle$ needs to be propagated in time. The propagation was performed in the position space $\psi_\ell^-(r) = \langle r|\Omega_\ell^-|\psi_\ell^i\rangle$ using the Chebyshev polynomial method [20], in time steps of δ_t. The time-correlation function $C_\ell(t)$ from Eq. (5) was then calculated by taking its overlap with the final scattering wave packet $\psi_\ell^+(r)$ at every time step, where δ_t was appropriately chosen to resolve $C_\ell(t)$ well, which is oscillatory in general.

A complex absorbing potential was used at the large r edge of the spatial grid, past where $\psi_\ell^+(r)$ is situated, to absorb the outward-propagating wave packet (after scattering) and prevent reflections that would otherwise interfere with the calculation. The calculation of $C_\ell(t)$ can be terminated when $|(e^{-iHt/\hbar}\psi_\ell^-)(r)| < \epsilon$, for some small enough ϵ (taken to be 10^{-9} here). This allows the calculation to run for a sufficiently long time, ensuring that all parts of the propagating wave packet have reached the asymptotic region, which is particularly important when the potential used supports resonances.

The momentum space wave function of the free wave packet was taken to be a complex Gaussian of the form

$$\chi_\ell^{f/i}(k) = (2\sigma_k^2\pi)^{-1/4} e^{-[(k-k_0)^2/(2\sigma_k)^2 \pm i(k-k_0)r_0]}, \qquad (9)$$

where $k_0, r_0 > 0$ define the central momentum and position of the free wave packets, respectively, and σ_k controls the momentum space width. Labels f/i on the parameters (σ_k, k_0, r_0) are taken implicitly on the RHS. As only the single-channel case is shown here, the initial scattering wave packet $\psi_\ell^-(r)$ was calculated and the final scattering wave packet was conveniently taken to be $\psi_\ell^+(r) = (\psi_\ell^-(r))^*$, to maximise the overlap in momentum space [6, 14], and thus range of $S_\ell(E)$.

4.2 Low energy $\alpha + \alpha$ scattering

The case of low-energy $\alpha + \alpha$ scattering with $\ell = 2$ was taken as an example, as it exhibits a well-known and well-defined low-energy resonance. The potential (of Woods-Saxon plus charged sphere Coulomb) was taken from Ref. [21]. The parameters for the free wave packets were taken to be $(\sigma_k, k_0, r_0) = (0.0417\,\text{fm}^{-1}, 0.536\,\text{fm}^{-1}, 880\,\text{fm})$. The k_0 used corresponds to the known resonance energy. σ_k was taken such that the wave packets are sufficiently narrow in momentum space to allow $|\chi_\ell^{f/i}(0)| \approx 0$. The large value of r_0 allows numerical calculation of Coulomb wave functions (which depend on kx) over the spatial range supported by the wave packets. A high spatial resolution of 10^{-2} fm was used to resolve the wave packet well and minimise errors in time propagation (performed in steps of $\delta_t = 1$ fm/c).

The calculated S-matrix, $S_\ell(E) \equiv e^{2i\delta_\ell(E)}$, is shown across Figs. 1a and 1c, along with equivalent calculations made using the static solver FRESCO [22]. The magnitude of the S-matrix agrees with unity to the level of $\sim 10^{-8}$ within the energy range $E(k_0 \pm 3\sigma_k)$ of the wave packet centre and within $\sim 10^{-4}$ for $E(k_0 \pm 6\sigma)$. The absolute difference in the nuclear phase shift $\delta_\ell^N \equiv \delta_\ell - \delta_\ell^C$ with respect to FRESCO is within $\sim 10^{-7} - 10^{-5}$ in this range. This demonstrates that the theoretical and numerical framework described above works well and allows the utilisation of essentially the entire range of energies supported by the wave packets to calculate $S_\ell(E)$.

The corresponding time-correlation function $C_\ell(t)$ has been shown in Figs. 1e and 1f. We can identify three distinct regions in time. (i) The initial scattering wave packet propagates into the interaction region and reflects back (outwards) to the asymptotic region after scattering, before overlapping with the final scattering wave packet ($C_\ell(t) \approx 0$). (ii) The outward-propagating wave packet then overlaps ($C_\ell(t) \gg 0$), initially forming a large peak from components that were reflected quickly. The latter contribution decays and (iii) is taken over by the exponentially decaying contribution from components temporarily trapped in the potential, which tunnel out of the barrier over time. In general, the larger the lifetime of the quasi-bound states formed, the more delayed the contribution from (iii) will be, resulting in a more prominent separation between the fast and slow mechanisms involved in the scattering. Further discussions can be found in Ref. [8].

Note that the feature appearing beyond region (iii) in Fig. 1f (at $t \approx 6.8 \times 10^4$ fm/c) may be attributed to reflections from the large r end of the spatial grid that have not been fully absorbed by the complex potential [8]. Such reflections of parts of the outward-propagating wave packet can cause them to re-scatter, increasing the noise in the results, particularly around resonance energies when the long-term decay of $C_\ell(t)$ is affected (cf. Fig. 1d).

4.3 The time-correlation function

Though we have not discussed it in great detail here, the time correlation function $C_\ell(t)$ can resolve different mechanisms (such as resonances) involved in scattering in time, and thus can be a useful object in separating the contribution from these mechanisms to the S-matrix. This object shows promise to be helpful in (i) interpreting the dynamics of the reaction and (ii) helping extract fusion observables using the model described in Sec. 1. While preliminary investigations were performed in Ref. [8], further work is required to determine the efficacy of this approach, and is aimed to be presented in a future publication.

Further, though here we have calculated the S-matrix by solving the time-dependent Schrödinger equation, we note that inverse mapping from the S-matrix to the time-correlation function is also possible:

$$S_\ell(E) \equiv \frac{(2\pi\hbar)^{-1}}{\alpha_\ell(E)} \int_{-\infty}^{\infty} \mathrm{d}t\, C_\ell(t) e^{iEt/\hbar} \qquad (10a)$$

$$\iff \quad C_\ell(t) = \int_0^{\infty} \mathrm{d}E\, \alpha_\ell(E) S_\ell(E) e^{-iEt/\hbar} \qquad (10b)$$

where $\alpha_\ell(E)$ describes the energy distribution of the wave packets. In principle, the time-correlation function may also be obtained from any calculation of $S_\ell(E)$, allowing a time-domain analysis of any system where static calculations are accessible. This could open a wide range of possibilities for studying the time dependence of few-body reactions using conventional static methods and solvers.

5 Summary

In summary, this work formally extends the application of the time-dependent wave packet approach to obtain the S-matrix using the time-correlation function to nuclear physics, where the Coulomb potential must be properly accounted for. The example of $\alpha + \alpha$ scattering was shown; results for elastic scattering of ^{16}O+^{208}Pb and ^{16}O+^{154}Sm can be found in Ref. [8], where similar accuracy was attained. This provides an accessible and accurate approach to solving time-dependent coupled channels (TDCC) problems. Furthermore, we highlight the usefulness of the time-correlation in resolving the time dependence of mechanisms involved in scattering and their contribution to the S-matrix.

In addition to the single-channel case, the forthcoming Ref. [9] will provide numerical examples for the multi-channel case to firmly establish the key concepts of the method. In future work, we will investigate the efficacy

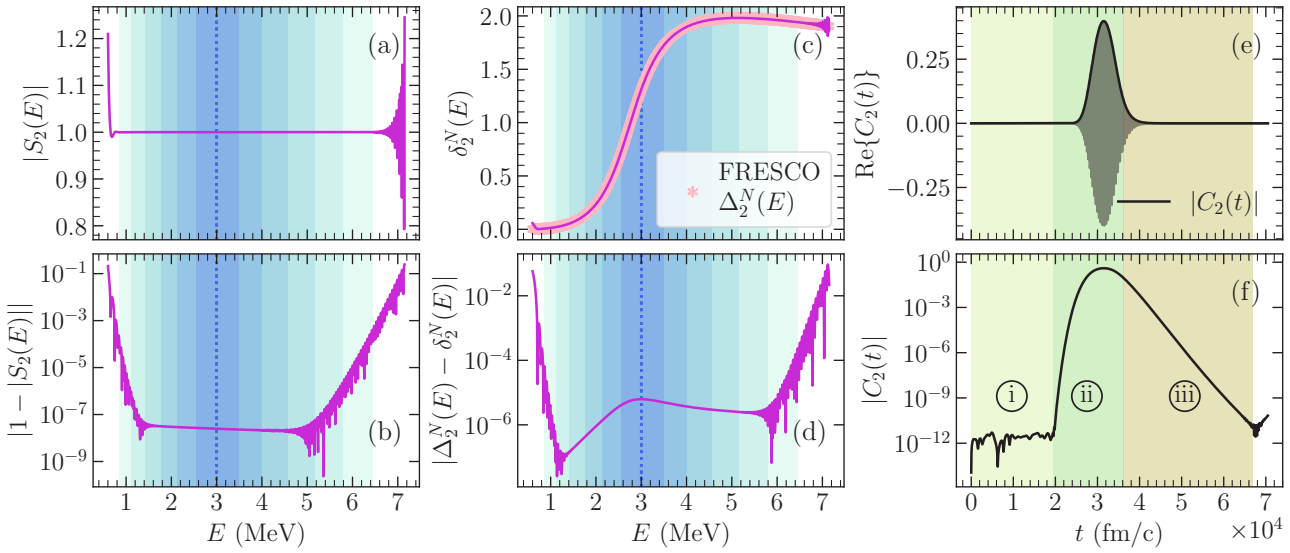

Figure 1: (a) The magnitude of the S-matrix $|S_2(E)|$, and (c) the nuclear phase shift $\delta_2^N(E)$ for low-energy scattering of two α particles as described in Sec. 4.2. (b) and (d) show respective errors for the magnitude of the S-matrix (compared to unity) and phase shift (compared to FRESCO, denoted $\Delta_2^N(E)$). In (a)–(d), dotted vertical lines mark $E(k_0)$ and the progressively shaded regions show $E(k_0 \pm n\sigma_k)$ for up to $n = 6$. The real part of the corresponding time-correlation function $C_2(t)$ is shown in (e), along with the magnitude, also given on a log scale in (f). In (e) and (f), the approximately shaded regions in time are described in Sec. 4.2. Calculation of $C_2(t)$ was terminated when condition in Sec. 4.1 was met.

of the fusion model introduced in Sec. 1, using the time-correlation function to obtain fusion observables. Since this may require a large number of channels, using TDCC may also offer computational advantages over static coupled channels approaches.

Acknowledgements

The authors acknowledge the support from the Australian Research Council Grant DP250101791. Helpful discussions with M. M. Webber on the computational methods are gratefully acknowledged.

References

[1] K. Hagino, K. Ogata, A. Moro, Coupled-channels calculations for nuclear reactions: From exotic nuclei to superheavy elements, Progress in Particle and Nuclear Physics **125**, 103951 (2022). 10.1016/j.ppnp.2022.103951

[2] K.J. Cook, D.C. Rafferty, D.J. Hinde, E.C. Simpson, M. Dasgupta, L. Corradi, M. Evers, E. Fioretto, D. Jeung, N. Lobanov et al., Colliding heavy nuclei take multiple identities on the path to fusion, Nat Commun **14**, 7988 (2023). 10.1038/s41467-023-43817-8

[3] A.C. Berriman, D.J. Hinde, M. Dasgupta, C.R. Morton, R.D. Butt, J.O. Newton, Unexpected inhibition of fusion in nucleus–nucleus collisions, Nature **413**, 144 (2001). 10.1038/35093069

[4] A. Mukherjee, D.J. Hinde, M. Dasgupta, K. Hagino, J.O. Newton, R.D. Butt, Failure of the Woods-Saxon nuclear potential to simultaneously reproduce precise fusion and elastic scattering measurements, Phys. Rev. C **75**, 044608 (2007). 10.1103/PhysRevC.75.044608

[5] M. Webber, Examining the onset of complexity in nuclear fusion using time-dependent coupled channels, Honours thesis, The Australian National University (2025)

[6] D.J. Tannor, D.E. Weeks, Wave packet correlation function formulation of scattering theory: The quantum analog of classical S-matrix theory, The Journal of Chemical Physics **98**, 3884 (1993). 10.1063/1.464016

[7] T. Vockerodt, A. Diaz-Torres, Calculating the S-matrix of low-energy heavy-ion collisions using quantum coupled-channels wave-packet dynamics, Phys. Rev. C **104**, 064601 (2021). 10.1103/PhysRevC.104.064601

[8] A.S. Tejas, Time-dependent wave packet scattering theory for asymptotically coulomb potentials with applications to nuclear collisions, Honours thesis, The Australian National University (2025), 10.25911/HM02-P702

[9] A.S. Tejas, E.C. Simpson (2026), manuscript in preparation

[10] J.D. Dollard, Quantum-mechanical scattering theory for short-range and Coulomb interactions, Rocky Mountain Journal of Mathematics **1**, 5 (1971). 10.1216/RMJ-1971-1-1-5

[11] S. Agmon, Spectral properties of Schrödinger operators and scattering theory, Annali della Scuola Normale Superiore di Pisa - Classe di Scienze, Serie 4, **2**, 151 (1975), numdam.org/item/ASNSP_1975_4_2_2_151_0.

[12] S.T. Kuroda, On a Paper of Green and Lanford, J. Math. Phys. **3**, 933 (1962). 10.1063/1.1724309

[13] I.J. Thompson, F.M. Nunes, Nuclear Reactions for Astrophysics: Principles, Calculation and Applications of Low-Energy Reactions, 1st edn. (Cambridge University Press, 2009), ISBN 978-0-521-85635-5 978-1-139-15215-0

[14] R. Viswanathan, S. Shi, E. Vilallonga, H. Rabitz, Calculation of scattering wave functions by a numerical procedure based on the Møller wave operator, The Journal of Chemical Physics **91**, 2333 (1989). 10.1063/1.457041

[15] D.E. Weeks, D.J. Tannor, A time-dependent formulation of the scattering matrix using Møller operators, Chemical Physics Letters **207**, 301 (1993). 10.1016/0009-2614(93)89004-2

[16] D. Marchesin, M.L. O'Carroll, Time-Dependent and Time-Independent Potential Scattering for Asymptotically Coulomb Potentials, J. Math. Phys. **13**, 982 (1972). 10.1063/1.1666098

[17] J. Dai, J.Z.H. Zhang, Time-Dependent Wave Packet Approach to State-to-State Reactive Scattering and Application to H + O2 Reaction, J. Phys. Chem. **100**, 6898 (1996). 10.1021/jp9536662

[18] H. Kröger, R.J. Slobodrian, Coulomb scattering of wave packets, Phys. Rev. C **30**, 1390 (1984). 10.1103/PhysRevC.30.1390

[19] T.A. Green, O.E. Lanford, III, Rigorous Derivation of the Phase Shift Formula for the Hilbert Space Scattering Operator of a Single Particle, J. Math. Phys. **1**, 139 (1960). 10.1063/1.1703644

[20] D. Xie, R. Chen, H. Guo, Comparison of Chebyshev, Faber, and Lanczos propagation-based methods for calculating resonances, J. Chem. Phys. **112**, 5263 (2000). 10.1063/1.481096

[21] L. Marquez, Alpha-alpha potential, Phys. Rev. C **28**, 2525 (1983). 10.1103/PhysRevC.28.2525

[22] I.J. Thompson, Coupled reaction channels calculations in nuclear physics, Computer Physics Reports **7**, 167 (1988). 10.1016/0167-7977(88)90005-6